

Available online at www.sciencedirect.com**ScienceDirect**

Procedia Engineering 132 (2015) 334 – 341

**Procedia
Engineering**www.elsevier.com/locate/procedia

The Manufacturing Engineering Society International Conference, MESIC 2015

Analysis of Ring Compression Test by Upper Bound Theorem as special case of non-symmetric part

A. Moncada^a, F. Martín^{a,*}, L. Sevilla^a, A.M. Camacho^b, M.A. Sebastián^b^a Department of Manufacturing Engineering, University of Malaga. C/ Dr. Ortiz Ramos, s/n E-29071 Málaga, Spain.^b Department of Manufacturing Engineering, Universidad Nacional de Educación a Distancia (UNED), c/ Juan del Rosal 12, 28040 Madrid, Spain.

Abstract

The ring compression test is considered one of the most reliable ways to obtain the friction shear factor existing in a plastic deformation process, particularly in open die forging processes. The test is performed on a ring-shaped specimen, so that the whole workpiece is axisymmetric. The application of the upper bound theorem with a triangular rigid zones model was initially developed with regard to plane strain and symmetrical geometric configurations. In this paper, the application to the ring faces consider that the neutral radius that defines the reversal of the flow of the material establishes two areas of different section and therefore the possibility of addressing the study considering not symmetrical sections.

© 2015 Published by Elsevier Ltd. This is an open access article under the CC BY-NC-ND license (<http://creativecommons.org/licenses/by-nc-nd/4.0/>).

Peer-review under responsibility of the Scientific Committee of MESIC 2015

Keywords: Ring Compression Test, Plastic Deformation, Upper Bound Theorem, Forging, Triangular Rigid Zones

1. Introduction

The ring compression test (RCT) is considered a reliable way to evaluate the friction existing in a process of plastic deformation. This type of test is valid in processes associated with an open die forge. Its contrasted development [1] leads to a series of results expressed in three graphs showing the friction coefficient of the inner diameter decreased of the ring and reducing the height of the specimen in question for each one of the three

* Corresponding author. Tel.: +34-951-952-309.
E-mail address: fdmartin@uma.es

canonical geometries established. These three canonical geometries facilitate different ratios between the outer and inner diameters and the height of the specimens under study (Table 1).

The main objective of this paper is to show the applicability of the upper bound theorem and its variant triangular rigid zones in the case of non-symmetrical parts. This approach is produced by considering the RCT from an empirical perspective in line with Avitzur's approach. The RCT is a known and proven test that compares favourably with those offered by the analytical method.

Table 1. Canonical forms in the RCT

Outer Diameter (Do)	Inner Diameter (Di)	Height (h)
6	3	2
6	3	1
6	3	0.5

The peculiarity of such configurations is that they provide the possibility to contrast the results obtained from tests with those from other analytical procedures such as the upper bound theorem (UBT), in particular by its application based on the triangular rigid zone (TRZ) model [2,3]. This application of the UBT is based on the consideration of plane strain, something perfectly acceptable if the proportions are the canonical ones referred to above.

The UBT is an analytical method of a potential high while to set the value of the load required to ensure the deformation of a piece in a plastic forming process with the ability to discriminate each of the energy components used. This can incorporate accurately the effect of both internal friction, caused by the distortion of plastic flow, and the existing external friction of the interface between tool and workpiece. The friction in processes in which the values of applied stresses are very high is mainly adhesion friction, denoted by shear factor m [4, 5].

The expression of UBT formulated by Prager and Hodge [6] (Eq. 1) indicates that, bearing in mind the existing surface discontinuities between the different rigid zones, among all possible kinematically admissible fields, the one that minimizes the expression:

$$J^* = \frac{2}{\sqrt{3}} \sigma_0 \int_V \sqrt{\frac{1}{2} \dot{\epsilon}_{ij} \dot{\epsilon}_{ij}} dV + \int_{S\Gamma} \tau |\Delta v| ds - \int_{S_t} T_i v_i ds \quad (1)$$

This is an expression in which deformation external energy (J^*) never has a higher value than that calculated from the above equation value. The first term expresses the energy consumed owed to the internal distortion of the deformation produced on the deformed body. The second term includes the energy produced by the shear discontinuity surfaces, including the contact area between tool and workpiece. The third term provides the energy consumed by any external tensile (or compressive) force that may occur in forming processes.

The TRZ model is established on the principle of plane strain whereby the flow of the material behaves as if it were composed of blocks where only rigid behaviour and the displacement occurs between shear surfaces at a speed associated with them [7-9] (Fig. 1) (where b corresponds to the width of a module of the same height h).

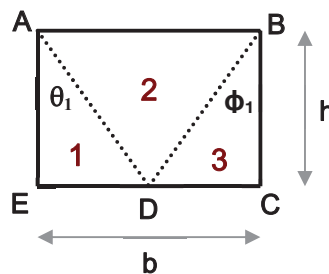


Fig. 1. TRZ Module.

The application of the model followed in this work corresponds to studies [2, 10] which consider a modular approach that establishes a basic module consisting of three TRZ. This module interacts with other existing modules via speeds input and output flow of deformed material, making the overall expression of Equation 1 in Equation 2:

$$\frac{dW}{dt} = \dot{W} = k \cdot \omega \cdot [\overline{AD} \cdot v_{12} + \overline{DB} \cdot v_{23} + \overline{AE} \cdot V_V + \overline{ED} \cdot m_2 \cdot v_1 + \overline{AB} \cdot m \cdot v_2 + \overline{CD} \cdot m_2 \cdot v_3] = P \cdot \omega \cdot b_1 \cdot V_v \quad (2)$$

UBT, usually applied in cases of symmetrical parts, or in any case with the possibility axisymmetric plane strain on considering the areas to be studied, usually perpendicular arrangement to the application of the yield strength. In the present case, the peculiar shape of the ring and the existence of a so-called neutral plane (NP), the plane establishing surface from which the material flows both in and out of the cylinder. This surface positions such that changes its position across the deformation process itself, allowing us to consider the sections studied as a particular case of non-symmetrical parts.

We have studied the application of UBT to axisymmetric parts for developing a method for determining the centre of mass, from which the modules that calculate the dimensionless ratio $p/2k$ (where p is the applied pressure, and k the shear stress of the material being studied). As shown in Figure 2 material flows plastically to the right and the left of the virtual vertical plane of separation of the piece, the so-called neutral plane. The determination of this neutral plane is given by the calculation of neutral radio by either of two alternatives. The first one employs the Avitzur equation [11, 12] (Equation 3) and the second is from own studies that calculate the centre of mass and integrate it directly into the equations with the dimensionless $p/2k$ relationship for a particular deformation range (Equations 4 and 5), where p is the applied pressure on the process surfaces and k the characteristic shear deformation of material. In any case, the NP will move from its initial position to the right or to the left depending on the friction since it modifies the evolution of the resulting deformation.

$$R_N = R_o \frac{2 \cdot \sqrt{3} \cdot m \cdot \left(\frac{R_o}{h} \right)}{\left(\frac{R_o}{R_i} \right)^2 - 1} \left[\sqrt{1 + \frac{\left(1 + \left(\frac{R_i}{R_o} \right) \cdot \left[\left(\frac{R_o}{R_i} \right)^2 - 1 \right] \right)}{2 \cdot \sqrt{3} \cdot m \cdot \left(\frac{R_o}{h} \right)}} - 1 \right] \quad (3)$$

$$\frac{p}{2k} = \frac{h_{CM}^2 + \left(\frac{X_{CM}}{2} \right)^2}{X_{CM} \cdot (h_{CM} + h_1)} + \left(\frac{h_1^2 + \left(\frac{X_{CM}}{2} \right)^2}{2 \cdot X_{CM} \cdot h_1} \right) * \left(1 - \frac{h_1 - h_{CM}}{h_1 + h_{CM}} \right) + m \cdot \frac{(h_1 - h_{CM})^2 + x_{CM}^2}{(2 \cdot x_{CM})(h_{CM} + h_1)} \quad (4)$$

$$\frac{p}{2k} = \frac{h_{CM}^2 + \left(\frac{b_2}{2} \right)^2}{b_2 \cdot (h_{CM} + h_1)} + \left(\frac{h_2^2 + \left(\frac{b_2}{2} \right)^2}{2 \cdot b_2 \cdot h_2} \right) \cdot \left(1 - \frac{h_{CM} - h_2}{h_{CM} + h_2} \right) + m \cdot \frac{(h_{CM} - h_2)^2 + b_2^2}{(2 \cdot b_2) \cdot (h_{CM} + h_2)} \quad (5)$$

For a non-symmetrical part, and as in the previous situation, it will be the neutral radio (NR) which determines the reversal in the direction of flow of the material (Figure 2) and from which we must establish the modules that implement the UBT.

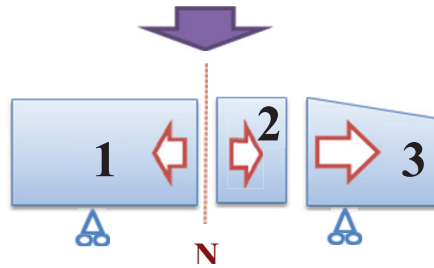


Fig. 2. Material flow of non-symmetrical pieces on the vertical plane (Neutral Plane, NP)

2. Methodology

In the particular case of a ring as used in the RCT, the height of the different modular sections generated will be the same because the specimen geometry maintains this constant thickness. This simplifies the calculation equations. Moreover, the application of UBT allows for the analysis for such a section representing a quarter of the total in the same condition that appropriate boundary conditions (Figure 3) are determined, as is the consideration of a horizontal symmetry with the flow of the material in the vertical direction is limited.

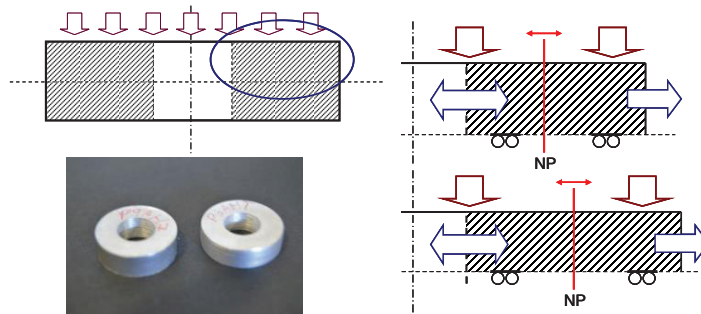


Fig. 3. Specimens analysed and ring section studied. Establishment of Neutral Plane (NP).

Therefore, the approach to the study of the load on the various samples tested is to be performed by the two alternatives given above. In the graph shown in Figure 4 contains two families of results obtained from the two criteria; The $p/2k_{xm}$ series denote those derived from the equations that calculate the centre of mass and no Modular approach maintained, ie, considering all the blocks that make up the section on a global basis. The second series called $p/2k_{xmM}$ is initialized with equation for calculating

Neutral Radio, and therefore determining the neutral position of the Neutral Plane, expressed by Avitzur [11].

A similarity can be seen in the evolution of the $p/2k$ to both criteria (Figure 4). In any case, since the modular approach offers slightly lower values, this criterion will be used in the implementation of the UBT (in addition to other advantages such as ease of deployment model). This paper presents a breakthrough in the application of UBT under this approach. Optimize the calculation of the required load [13] from the variation of the number of modules configured in sections on either side of Neutral Plane.

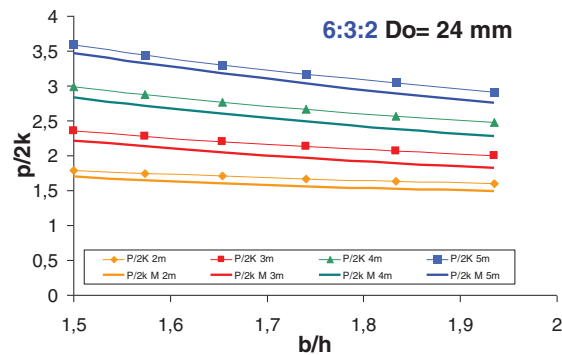


Fig. 4. Results obtained for $p/2k$ for different approaches.

The acceptability of a non-symmetrical specimen to a kind of general piece, virtually no geometric constraints exist. In this case non-consideration of the symmetrical part allows the study of the flow of the material incorporating the effect of friction calculated from the RCT.

3. Results and discussion

A large number of cases corresponding to the three canonical relations in the RCT trials (Table 1) are listed in Table 2.

Table 2. Analysed cases

Canonical relationship (Do:Di:h)	6:3:2	6:3:1	6:3:0.5
Do (mm)	120	120	120
Do (mm)	60	60	60
Do (mm)	24	24	24
Do (mm)	18	18	18
Do (mm)	12	12	12

Among the cases studied, different geometric configurations are progressively analysed, and with the same total width of the section under study, have been added module to module. The distortion of the modules can be greater or smaller in each case depending on the aspect ratio (width of the section / height of the section) (Figure 5).

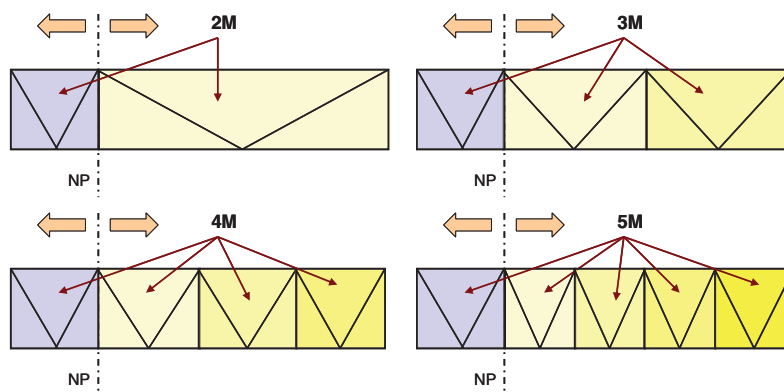


Fig. 5. Optimization by increasing modules.

A last column in each table (Tables 5 to 7) is included where the minimum values correspond to each of the alternatives (2M, two modules; 3M, three modules; 4M, four modules; 5M five modules) and comprise the minimum line, i.e., the optimum curve that meets the minimum values of $p/2k$ in the overall development process. The values in the tables and others that have been incorporated have been processed and treated graphically as shown in Figs. 6 to 8 to realize the evolution and load requirements in each situation.

As a result, therefore it shows alternatives of 15 different sizes of parts, retaining the ratios (and hence, the inside diameter and height of the rings) with outer diameters ranging from 12 to 120 mm (Tables 3 to 5 and Figs. 6 and 7).

Table 3. Values of $p/2k$ to 6: 3: 2 ratio and $Do = 24$ mm.

b/h	P/2k 2M	P/2k 3M	P/2k 4M	P/2k 5M	P/2k min
1.5	1.70	2.21	2.83	3.47	1.70
1.58	1.65	2.13	2.71	3.32	1.65
1.66	1.60	2.05	2.60	3.17	1.60
1.74	1.56	1.97	2.48	3.03	1.56
1.84	1.52	1.89	2.38	2.89	1.52
1.94	1.49	1.82	2.27	2.76	1.49

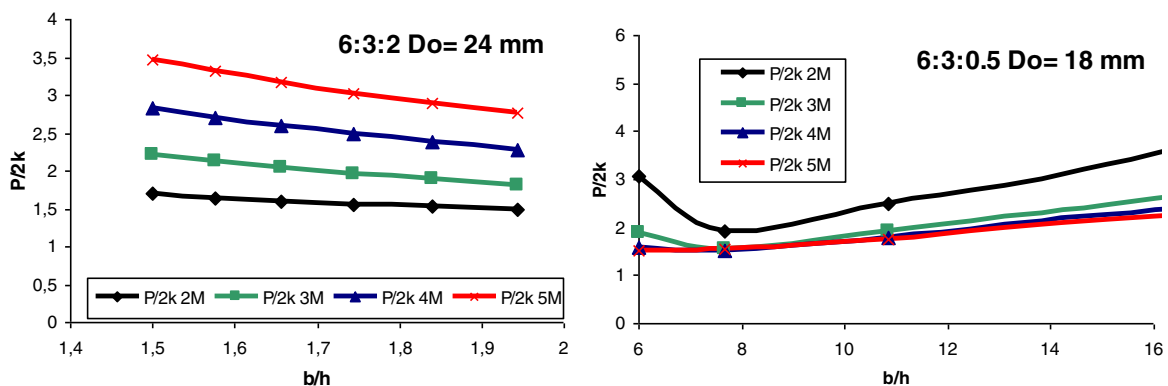


Fig. 6. Values of $p/2k$: (a) 6:3:2 relation; $Do = 24$ mm (b) 6:3:0.5 relation; $Do = 18$ mm

In this case (Figure 6a), ratio 6: 3: 2 and specimens with 24 mm outer diameter (Do) is observed in any of the solutions proposed curve minimum (optimum) is achieved throughout the process if they are considered two modules, two on each side of neutral plane (NP).

In Figure 6b different optimal configurations such as 4M (three modules in one section) and 5M (four modules in the same section) for different form factors appear.

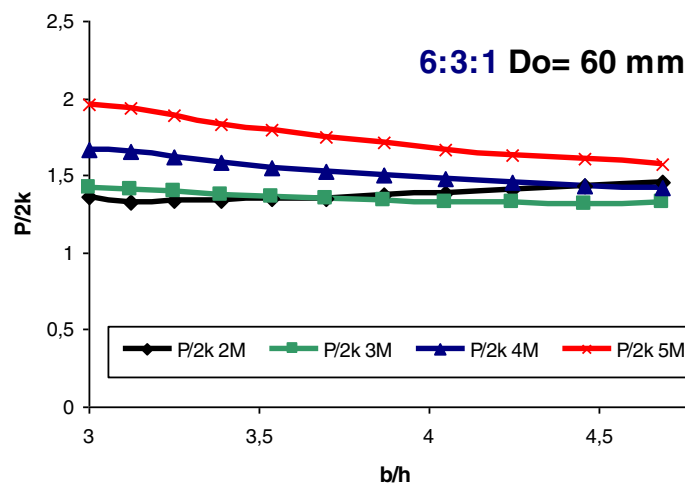
Table 4. Values of $p/2k$ ratio of 6: 3: 0.5 and $Do = 18$ mm.

b/h	P/2k 2M	P/2k 3M	P/2k 4M	P/2k 5M	P/2k min
6	3.07	1.87	1.58	1.52	1.52
7.69	1.91	1.55	1.52	1.57	1.52
10.83	2.50	1.91	1.78	1.76	1.76
16.56	3.67	2.67	2.38	2.26	2.26
31.05	8.21	4.61	3.43	2.85	2.85

Table 5. $p/2k$ results of 6: 3: 1 ratio and $D_o = 60$ mm.

b/h	P/2k 2M	P/2k 3M	P/2k 4M	P/2k 5M	P/2k min
3	1.37	1.42	1.67	1.95	1.37
3.12	1.33	1.41	1.65	1.93	1.33
3.39	1.34	1.37	1.58	1.84	1.34
3.87	1.37	1.34	1.50	1.71	1.34
4.05	1.38	1.33	1.47	1.67	1.33
4.25	1.40	1.32	1.45	1.63	1.32
4.69	1.46	1.32	1.42	1.57	1.32

The last cases presented in this paper are the 2M (1 Module section) and 3M (2 Modules section). The different configurations of modules provide the minimum value and therefore the optimum.

Fig. 7. $P/2k$ results of 6: 3: 1 ratio and $D_o = 60$ mm.

4. Conclusions

The analysis of the plastic deformation of a ring subjected to a process of forge as in the case of RCT is considered here and studying sections which have similar development to those on a piece with non-symmetrical geometry has allowed a new approach to implementing the upper bound theorem by means of a TRZ application.

The UBT calculation method is a limit derived from analysis, calculated to achieve load deformation of the workpiece substantially greater than the real one. It is therefore interesting to calculate a method to optimize and get smaller values in the approach to real values mentioned above. The alternative proposed to achieve this optimization is based on various configurations of modules for the same section.

Different cases presented show the advantage of such variation in the arrangement of modules. A curve is clearly established through which there is minimum on the evolution in the load to optimally achieve its value. The distortion to which modules are subjected depends on the form factor (b/h) and implies the minimum values of p from a section formed by a single module to be formed by four.

Acknowledgements

The authors want to thank the University of Malaga – Andalucia Tech, International Campus of Excellence, and the FPU program of the Ministry of Education, Culture and Sport of Spain for its economic contribution on this paper.

References

- [1] AA. VV. ASM Handbook, Forming and Forging. ASM International. 14, Metals Park, Ohio, USA (1996).
- [2] F. Martin, L. Sevilla, M.A. Sebastián. Implementation of Technological and Geometrical Parameters in Forging Processes by Means of the Upper Bound Element Technique. American Institute of Physics Conference Proceedings, 1181 (2009), pp. 455-463.
- [3] F. Martin. Development, integration and optimization at the study of forging processes by the Upper Bound Theorem through Triangular Rigid Blocks model. PhD. Thesis. University of Malaga. Malaga. Spain 2009.
- [4] S.B. Petersen and P. Martins. An alternative ring-test geometry for the evaluation and friction under low normal pressure. Journal of Materials Processing Technology, 79 (1998), pp. 14-24.
- [5] T. Altan and C.H. Lee. Influence of Flow Stress and friction Upon Metal Flow in Upset Forging of Rings and Cylinders. Journal of Engineering for Industry. Transactions of the ASME. 94 (3), (1972), pp. 775-782.
- [6] W. Prager and P.G. Hodge. Theory of Perfectly Plastic Solids. Chapman & Hall, Ltd., London, 1951.
- [7] J. Chakrabarty, Theory of plasticity, Elsevier Science, Oxford (U.K.), 2006.
- [8] F. Martin, L. Sevilla, E. Rubio, M.A. Sebastián. Bases para la aplicación del Teorema del Límite Superior en procesos de forja sobre configuraciones geométricas modulares. Proc. of MESIC 2007: 2nd Manufacturing Engineering Society International Conference. Madrid, Spain, 2007.
- [9] E.M. Rubio. Energetic analysis of tube drawing processes by the Upper Bound Method using theoretical work-hardening materials. Steel Research International, (2012), pp. 555-558.
- [10] F. Martin, A.M. Camacho, R. Domingo, L. Sevilla. Modular Procedure to improve the application of the Upper Bound Theorem in forging. Materials and Manufacturing Processes. (DOI: 10.1080/10426914.2012.718478).
- [11] B. Avitzur and C.J. Van Tyne. Ring Forming: An Upper Bound Approach. Part 1: Flow Pattern and Calculation of Power. Journal of Engineering for Industry. Transactions of the ASME. 104, pp. 231-237.
- [12] B. Avitzur. Metal forming: Processes and analysis. Robert E. Krieger Publishing Company, Inc. Huntington, New York, USA (1968).
- [13] H. Hung-Hsiou and T. Gow-Yi. Two analytical models of double-layer clad sheet compression forming based on the upper bound and the slab methods. Journal of Materials Processing Technology, 140 (2003), pp 604-609.